Prediction of the unknown: Inspiring experience with the CAPRI experiment

ARTICLE *in* PROTEINS STRUCTURE FUNCTION AND BIOINFORMATICS · JULY 2003

Impact Factor: 2.63 · DOI: 10.1002/prot.10392 · Source: PubMed

5 AUTHORS, INCLUDING:

Efrat Ben-Zeev
Weizmann Institute of Science
14 PUBLICATIONS **270** CITATIONS
SEE PROFILE

Alexander Heifetz
23 PUBLICATIONS **519** CITATIONS
SEE PROFILE

Miriam Eisenstein
Weizmann Institute of Science
164 PUBLICATIONS **5,872** CITATIONS
SEE PROFILE

PROTEINS: Structure, Function, and Genetics 52:41–46 (2003)

Prediction of the Unknown: Inspiring Experience With the CAPRI Experiment

Efrat Ben-Zeev,[1] Alexander Berchanski,[1] Alexander Heifetz,[1] Boaz Shapira,[1] and Miriam Eisenstein[2]*
[1]*Department of Biological Chemistry, The Weizmann Institute of Science, Rehovot, Israel*
[2]*Chemical Services, The Weizmann Institute of Science, Rehovot, Israel*

ABSTRACT **We submitted predictions for all seven targets in the CAPRI experiment. For four targets, our submitted models included acceptable, medium accuracy predictions of the structures of the complexes, and for a fifth target we identified the location of the binding site of one of the molecules. We used a weighted-geometric docking algorithm in which contacts involving specified parts of the surfaces of either one or both molecules were up-weighted or down-weighted. The weights were based on available structural and biochemical data or on sequence analyses. The weighted-geometric docking proved very useful for five targets, improving the complementarity scores and the ranks of the nearly correct solutions, as well as their statistical significance. In addition, the weighted-geometric docking promoted formation of clusters of similar solutions, which include more accurate predictions. Proteins 2003;52:41–46.** © 2003 Wiley-Liss, Inc.

Key words: weighted docking; clusters; conserved surface patches; blind predictions; protein–protein interactions

INTRODUCTION

In the past two decades we witnessed the emergence of a large variety of theoretical algorithms designed to predict the structures of protein–protein and protein-ligand complexes (docking). Such predictions can be performed at several levels. The most accurate predictions aim to identify in detail the intermolecular interactions and to estimate the energy of binding. The least accurate predictions aim to identify the interaction site on one or both molecules. Even these low-accuracy predictions often provide valuable information that can be used for analysis of experimental data and for planning of new experiments.

The CAPRI experiment concentrates on a small number of prediction targets, whose structures are not known, and all the groups participating in the experiment study the same targets. In this way, two important factors, which make a comparison of the performance of different algorithms difficult, are eliminated: the choice of targets, which may be harder or easier for prediction, and the bias, which is naturally introduced when the predictor knows the expected results.

We submitted predictions for all seven targets in the CAPRI experiment. Once the experimental structures were released, we found that for four targets our submitted predictions included a nearly correct structure, and for a fifth target we predicted the binding site of one of the molecules but not of the other. Further analysis of our predictions provided a wealth of information concerning newly designed modifications, assumptions, and approximations in our approach, some of which proved more adequate than other ones.

MATERIALS AND METHODS

Our prediction algorithm has been described before in several publications.[1–3] It involves digitization of the molecules, distinguishing the surface from the interior, and correlation of the three-dimensional representations via fast Fourier transformations. Higher correlation values (scores) reflect better complementarity. In the CAPRI predictions we used a new version of our program MolFit, which allows weighted-geometric docking.[4] The weighing scheme was matched to the specific target and depended on information from biochemical experiments or from our bioinformatics studies.

The general prediction procedure included the following steps (details particular to each target are given in Table I):

1. Water molecules, ions, and sugars were omitted from the lists of coordinates. A weighted-geometric search was performed, in which the whole rotation-translation space was scanned (global scan) or a part of it (partial scan). An angular interval of 12° was used in the global scans, whereas in the partial scans a finer interval of 9° was used. The translation intervals were 1.1–1.2 Å. In addition, a geometric scan was performed to obtain an estimate of the effect of weighing. The solutions in each scan were sorted by their complementarity scores. We did not use geometric-electrostatic docking because the pairs of molecules did not present large electrostatic surface patches, necessary to make such a docking search advantageous[3] (except in target 1, see below).
2. An extreme value distribution function[5] was fitted to

E.B.Z., A.B., A.H., and B.S. contributed equally and are listed in an alphabetical order.

*Correspondence to: Miriam Eisenstein, Department of Chemical Services, The Weizmann Institute of Science, Rehovot 76100, Israel. E-mail address: miriam.eisenstein@weizmann.ac.il

Received 29 October 2002; Accepted 16 December 2002

TABLE I. Prediction Procedures Used for Producing the Models Submitted to CAPRI

Target	Preparation of the starting structures	Weighing scheme	Scanning mode: Starting positions	Scanning mode: Scanning range and additional details	Filtering particulars
T01: HPrK–HPr	Only a trimer of HPrK was considered. The missing loop HPrK/241–252 was modeled.[a] Missing atoms in exposed side-chains of HPrK were completed. Different conformations were given to the side-chains of H140 and R206 in each subunit in the trimer.	HPrK: up-weighting the side-chains of S157, E163, D179, I210, T294, and F297 ($t = 1$).[b] HPr: up-weighting the side-chains of D46 and I47.[c]	The up-weighted residues of HPrK and HPr faced one another.	A partial scan in the range 0–360° about the HPrK threefold axis and ±54° about the perpendicular axes. Exposed lysines in both molecules were trimmed.[d]	Residue D46 of HPr was required to point generally in the direction of the HPrK P-loop.
T02 and T03: VP6-antibody and HA-antibody	VP6 and HA were cut perpendicularly to their threefold axes[e] leaving about 2/3 of the molecule, which includes the antigenic sites.[f,g] Only the Fv fragment of the antibody was considered.	Antibody: up-weighting the exposed side-chains in the CDRs ($t = 0.8$).	The approximate twofold of the Fv was aligned with the threefold of VP6 or HA.	A partial scan as for T01. Docking to the artificial surfaces of VP6 and HA (formed by the cutting of the molecules) was prevented.[h]	None.
T04, T05, T06: α-amylase-camelid antibody	Two structures of α-amylase were used in the docking searches (PDB codes 1pif, 1dhk) with the largest variation in the flexible loops.[i]	Antibody: up-weighting the exposed side-chains of the CDRs ($t = 1$).	As sent by the CAPRI team.	Global scan. The exposed lysines of α-amylase were trimmed.[d]	Models with more than 4 non-CDR contacts[j] were eliminated.
T07: TCRβ-toxin	Only one domain of TCRβ was considered (residues R3–R116).	TCRβ: down-weighting side-chains that interact with the α chain[k] ($t = -0.5$).	As sent by the CAPRI team.	Global scan.	The solution that resembled 1jck[l] was ranked 1st.

[a]The loop was modeled on the basis of weak sequence similarity to a loop in adenosine 5′-phosphosulfate kinase[6] (PDB[7] code 1d6J).
[b]Residues H140, E204, and R206, which are a part of the conserved patch but were modeled by us, were not up-weighted.
[c]Residue M48, which is a part of the conserved patch but may change conformation on ligand binding,[8] was not up-weighted.
[d]The trimming procedure is described by Heifetz and Eisenstein.[33]
[e]The large VP6[9] and HA[10] molecules were cut because of our limited CPU and not because of algorithmic limitations.
[f]The antigenic site of VP6 is known[11]; we were not aware of the low-resolution structure of VP6/Fab-238[12] when the predictions were made.
[g]The antigenic regions of HA are confined to a limited part of the molecule.[13,14]
[h]We treated the artificial surfaces as if they were a part of the interior of the molecule.[3]
[i]Loops 304–310 and 347–353 of α-amylase change conformation when a ligand binds.[15,16]
[j]Despite the weighing scheme, many top ranking solutions had contacts involving non-CDR residues (distance < 4.0 Å), which are not common in known protein-camelid antibody structures.[17–20]
[k]Based on the structure of the human α,β TCR.[21]
[l]The portion of the TCRβ in another TCRβ/toxin complex[22] (PDB code 1jck), which is in contact with the toxin, is almost identical to the corresponding fragment in the TCRβ in target 7 in terms of sequence and structure, including most of the side-chain conformations. The toxin in target 7 has a flexible loop.[23,24] However, superposition on the toxin in 1jck shows that this loop is not at the binding interface.

the observed distribution of scores in each scan, providing estimates of the mean score and the standard deviation (σ) for the scan and the statistical significance, Z, for each solution.[3]

3. Approximately 100 top ranking solutions (top 2.5–4σ) from each scan were filtered (see Table I), clustered, and manually analyzed. Clusters were formed according to the predicted interactions at the interface, requiring that at least 50% of the residue–residue contacts are the same. Each cluster was represented by the highest scoring solution within it, because in this solution there are fewer intermolecular clashes. The manual viewing was used to eliminate severe clashes and to estimate qualitatively the possibility of ion pair and hydrogen bond formation across the interface.
4. Good putative solutions were refined by small rigid body rotations of $\pm 2°$ around the position obtained in the scan.
5. The predicted models were submitted to CAPRI ordered by their weighted complementarity scores after the refinement, except for targets 3 and 7 (see below).

We estimate the accuracy of our predictions by calculating the root-mean-square deviation (RMSD) between the Cα atoms of the "ligand" (the smaller molecule in the complex) in the predicted and experimental structures, after superposition of the larger molecule. The statistical significance of a given solution is measured by its ΔZ value, which is the difference (in σ units) between the Z value of this solution and the Z value of the solution with the highest score in that scan. Unlike the complementarity scores, which depend on the system, the grid interval and the weighing scheme, the Z values are normalized with respect to the other solutions in the scan, providing a means of comparison between different scans.

RESULTS

Target 1-HPr Kinase (HPrK)-HPr

We calculated multiple-sequence alignments for HPrK and HPr with ClustalW[25] and identified the conserved (or mostly conserved) residues. Mapping these residues on the molecular surfaces distinguished patches as follows. In HPrK, the conserved patch included nine residues from neighboring subunits (see Fig. 1). In HPr, it comprised residues I47, M48, and S46, where phosphorylation or dephosphorylation by HPrK is expected. We assumed that the conserved patches correspond approximately to the interacting surfaces and up-weighted the contacts between them (see Table I). Notably, HPr has a large negative potential patch around H15, which is its phosphorylation site, but not by HPrK. We did not include electrostatic complementarity in this case to avoid formation of false-positive solutions in which H15 is involved. In addition, the available structures of HPrK[26] and HPr[27] are from different species, and use of the electrostatics, which depends on the amino acid sequence, is likely to introduce errors.

The solution that we submitted as first to CAPRI is acceptable (see Table II). It is interesting that in all our submitted solutions, the location of HPr, which is dictated by the weighing scheme, is approximately correct (displacements of 1.1–5.1 Å, as calculated by the assessors). Thus, the assumption that the conserved patch on the surface of HPrK is involved in HPr recognition was correct. Inspection of our scan data indicated that the nearly correct prediction was at the edge of the partial search range. Therefore, we performed a global scan, using the same weighting scheme. This scan produced a considerably more accurate prediction, with an RMSD of 4.5 Å from the experimental structure[28] compared to 8.1 Å for the submitted prediction.

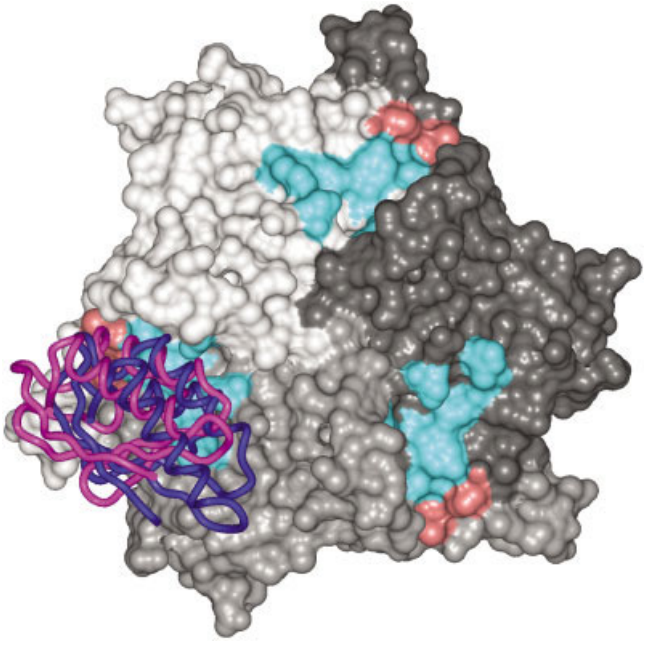

Fig. 1. Superposition of the predicted and the experimental positions of HPr in target 1. The surfaces of three subunits of HPrK are colored in different shades of gray. The conserved residues T294 and F297 are colored in red, and the conserved residues H140, S157, E163, D179, E204, R206, and I210 are colored in cyan, showing that the conserved surface patch is formed from residues in neighboring subunits. The position of HPr in the experimental structure is depicted by the blue ribbon and in our prediction by the magenta ribbon.

What if we did not model the missing loop HPrK-241-252 (see Table I)? While preparing the solutions for CAPRI, we performed two additional partial scans, one in which the modeled loop was down-weighted and another in which this loop was omitted. In both scans, the acceptable solution had a lower complementarity score and lower ΔZ values (-4.3 and -5.5 vs -2.5σ for the submitted solution). Hence, although most of the contacts between the modeled loop and HPr are probably incorrect, they add to the complementarity score of the acceptable solution without forming additional false-positive solutions.

Target 2-VP6-Antibody

Two solutions, ranked 1 and 3 in the partial scan, were singled out by their high weighted-geometric complementarity scores. The refinement improved the weighted score of solution 3 significantly above that of solution 1. In

TABLE II. Prediction Results.†

Target	Scan type	No. of clustered solutions	Rank and deviations of the nearly correct solution in the CAPRI assessment.	Rank (in the scan), ΔZ, and RMSD of the nearly correct solution[a]	Rank and size[b] of the cluster that includes the nearly correct solution	Rank, ΔZ, and RMSD of the most accurate solution in the cluster
T01: HPrK-HPr	Partial; Weighted	118 (top 4σ)	1,33.3°, 5.1 Å	16, −2.5σ, 8.1 Å	1,10	92, −3.7σ, 7.1 Å
	Partial; Geometric			312, −4.0σ, 8.1 Å		
	Global; Weighted	140 (top 4σ)		6, −1.3σ, 4.5Å	1, 7	36, −2.9σ, 4.1 Å
T02: VP6-antibody	Partial; Weighted	144 (top 3σ)	1, 15.5°, 7.5 Å	3, −0.2σ, 6.7 Å	1,13	39, −2.0σ, 1.0 Å
	Partial; Geometric			307, −4.0σ, 6.7 Å		
	Global; Weighted	263 (top 3σ)		28, −1.3σ, 7.0 Å	4,15	120, −2.4σ, 2.8 Å
T03: HA-antibody	Partial; Weighted	88 (top 3σ)	10[c], 17.3°, 2.7 Å	1, 0.0σ, 5.8 Å	1,20	10, −1.8σ, 2.5 Å (LH)[d] 22, −2.1σ, 1.5 Å (UT)
	Partial; Geometric			77, −4.6σ, 5.8 Å		
	Global; Weighted	174 (top 3σ)		1, 0.0σ, 4.7 Å	1,21	83, −2.6σ, 1.3 Å (LH)[d] 133, −2.7σ, 1.8 Å (UT)
T04: α-amilase-camelid antibody	Global; Weighted[e]	209 (top 2.5σ) 73 (top 3σ)	None			
	Global; Geometric			732, −5.5σ, 9.7 Å		
T05: α-amilase-camelid antibody	Global; Weighted[e]	86 (top 4σ) 105 (top 3σ)	None			
	Global; Geometric			>1000		
T06: α-amilase-camelid antibody	Global; Weighted[e]	155 (top 2.5σ) 57 (top 4σ)	None	1, 0.0σ, 1.2 Å	1, 7	1, 0.0σ, 1.2 Å
	Global; Geometric			4, −0.7σ, 4.9 Å		
T07: TCRβ-toxin	Global; Weighted	214 (top 5σ)	1, 3.9°, 1.3 Å	109, −3.9σ, 7.2 Å	7, 5	214, −4.5σ, 6.9 Å
	Global; Geometric			962, −5.3σ, 7.2 Å		

The first line for each target lists data for the models submitted to CAPRI.
[a]ΔZ and RMSD are defined in Materials and Methods.
[b]The size of the cluster is the number of similar solutions within it, including symmetry-related solutions.
[c]We submitted 10 solutions to CAPRI in reversed order.
[d]There are two HA-antibody complexes in the asymmetric unit,[29] with antibody chain identifiers LH and UT.
[e]Results of two scans are given of the antibody docked to 1pif or 1dhk, respectively.

addition, solution 3 had a higher geometric score, suggesting fewer intermolecular clashes, and therefore, this solution was ranked 1st among the solutions submitted for assessment. This prediction is close to the experimental structure (see Table II) with an RMSD of 6.7 Å. Another prediction, which we ranked 3rd in the CAPRI submission, had a few more correct intermolecular contacts (24 vs 20), but it deviated more from the experimental structure (RMSD of 12.6 Å) and had more clashes.

The results of the global weighted-geometric scan are somewhat worse than those of the corresponding partial scan (see Table II), possibly because of the larger angular interval. Nevertheless, both weighted scans give much better results than the partial geometric scan, supporting the weighing scheme.

Target 3-Hemagglutinin (HA)-Antibody

Our 10th submitted prediction is acceptable (see Table II), with an RMSD of 5.8 Å from the experimental structure[29] (our solutions were submitted in reversed order by mistake). We also submitted a less accurate solution (RMSD of 12.7 Å) ranked 2nd. Nearly correct solutions were ranked 1st in both, the partial and the global weighted-geometric scans, whereas in the partial geometric scan, the rank was much lower. Again, the weighing scheme proved very successful.

Targets 4, 5, and 6-α-Amylase-Camelid Antibody

None of the solutions submitted by us for targets 4, 5, and 6 is acceptable. The antibodies in targets 4 and 5 do not bind via their CDRs, and one tends to relate our failure to predict these structures to the weighing scheme. To test this notion, we compared our predictions from the geometric scans to the experimental structures.[30] For target 4, we found an acceptable solution (RMSD of 9.7 Å) ranked 732, but for target 5, an acceptable solution was not found among the top 1000 solutions. Geometric docking of the bound conformations for targets 4 and 5 identified correct solutions ranked 3 ($\Delta Z = -0.1$) for target 4, and 10 ($\Delta Z = -2.3$) for target 5. Hence, even in bound docking, the statistical significance of the correct solution for target 5 is relatively low.

In contrast to targets 4 and 5, our geometric docking identified an acceptable solution for target 6, ranked 4. In the weighted-geometric docking, an acceptable solution is ranked 1, but it was discarded in the filtering step. Obviously, the filtering procedure was too demanding. It is interesting that our geometric docking results for targets 4–6 follow the antibody-α-amylase-binding constants[30]: a good, high-ranking, prediction for target 6 (KD = 3.5 ± 1.4 nM), a poorer prediction for target 4 (KD = 24 ± 4 nM), and no prediction for target 5 (KD = 232 ± 7 nM).

Target 7-TCRβ-Toxin

Our first submitted solution is nearly correct (see Table II) with an RMSD of 7.5 Å from the experimental structure.[31]

DISCUSSION

Our group submitted predictions for all seven targets, including acceptable predictions for targets 1, 2, 3, and 7, and a prediction of the binding position of the antibody in target 6. The predictions are of medium accuracy; hence, the RMSD values range from 5.8 Å for target 3 to 8.1 Å for target 1 (see Table II). Nevertheless, many of the intermolecular contacts are correctly predicted and can be used for analysis and design of experiments.

Notably, the acceptable solutions are within clusters of similar predictions, especially in the weighted-geometric searches (see Table II). We represented each cluster by the highest scoring solution; however, more accurate predictions can often be found. We are currently designing and testing several clustering approaches in an attempt to find a better definition and a better representation of the clusters. It is interesting that target 3 stands out with a very large cluster, which includes solutions similar to both experimental complexes. One is tempted to speculate that the size of the cluster represents a genuine characteristic of the interacting surfaces, which in target 3 are more accommodating than the common notion of tight lock-and-key binding.

An important feature of our algorithm is the option to up-weight or down-weight contacts involving specific residues in one or both molecules. It proved very successful for targets 1, 2, 3, 6, and 7 (comparison with geometric docking results is given in Table II). Moreover, the statistical significance of the acceptable solutions in the weighted scan is high, usually within the top 2.5σ range. Postscan filtering of the solutions is an alternative approach to our weighted-geometric docking. However, if a given solution is not found in the output list, a filter cannot fish it out. In addition, the formation of clusters of solutions is by far more effective in the weighted scans. The decision on which residues should be up-weighted depends on our knowledge of the system. In this CAPRI experiment, there were six targets that included antibodies or TCRs, whose binding characteristics have been studied in detail. For HPrK-HPr (target 1), we successfully tested another approach, which suggests that conserved surface patches are likely to have biological significance.[32]

For three targets, we compare the results of a partial scan with an angular interval of 9° to results of a global scan with a 12° interval. Despite the finer grid, the partial scan forms a slightly more accurate prediction only for target T03.

CONCLUSIONS

The CAPRI experiment provided grounds for testing different modifications of our algorithm, such as weighted-geometric docking, partial scanning of the rotation space, and clustering of solutions. We find that weighted-geometric docking and clustering are particularly useful. In addition, in the one tested case, weights derived from amino acid conservation patterns in homologous proteins are adequate, although the definition of the binding site is partial and approximate. In contrast, limiting the search to a predefined range of angles shortens the computations,

but it does not help to eliminate false-positive solutions and is a severe drawback when the search range is inadequate (see results for T01).

ACKNOWLEDGMENTS

We thank the organizers of CAPRI, the assessors, the contributors of prediction targets, and the participants for two hectic and inspiring prediction periods. We thank Professor Ephraim Katchalski-Katzir for his support throughout this study.

REFERENCES

1. Katchalski-Katzir E, Shariv I, Eisenstein M, Friesem AA, Aflalo C, Vakser IA. Molecular surface recognition: determination of geometric fit between proteins and their ligands by correlation techniques. Proc Natl Acad Sci USA 1992;89:2195–2199.
2. Eisenstein M, Shariv I, Koren G, Friesem AA, Katchalski-Katzir E. Modeling supra-molecular helices: extension of the molecular surface recognition algorithm and application to the protein coat of the tobacco mosaic virus. J Mol Biol 1997;266:135–143.
3. Heifetz A, Katchalski-Katzir E, Eisenstein M. Electrostatics in protein-protein docking. Protein Sci 2002;11:571–587.
4. Ben-Zeev E, Eisenstein M. Weighted geometric docking: incorporating external information in the rotation-translation scan. Proteins 2003;52:24–27.
5. Levitt M, Gerstein M. A unified statistical framework for sequence comparison and structure comparison. Proc Natl Acad Sci USA 1998;95:5913–5920.
6. MacRae IJ, Segel IH, Fisher AJ. Crystal structure of adenosine 5′-phosphosulfate kinase from Penicillium chrysogenum. Biochemistry 2000;39:1613–1621.
7. Berman HM, Westbrook J, Feng Z, Gilliland G, Bhat TN, Weissig H, Shindyalov IN, Bourne PE. The Protein Data Bank. Nucleic Acids Res 2000;28:235–242.
8. Najmanovich R, Kuttner J, Sobolev V, Edelman M. Side-chain flexibility in proteins upon ligand binding. Proteins 2000;39:261–268.
9. Mathieu M, Petitpas I, Navaza J, Lepault J, Kohli E, Pothier P, Prasad BV, Cohen J, Rey FA. Atomic structure of the major capsid protein of rotavirus: implications for the architecture of the virion. EMBO J 2001;20:1485–1497.
10. Sauter NK, Hanson JE, Glick GD, Brown JH, Crowther RL, Park SJ, Skehel, JJ, Wiley DC. Binding of influenza virus hemagglutinin to analogs of its cell-surface receptor, sialic acid: analysis by proton nuclear magnetic resonance spectroscopy and X-ray crystallography. Biochemistry 1992;31:9609–9621.
11. Tang B, Gilbert JM, Matsui SM, Greenberg HB. Comparison of the rotavirus gene 6 from different species by sequence analysis and localization of subgroup-specific epitopes using site- directed mutagenesis. Virology 1997;237:89–96.
12. Thouvenin E, Schoehn G, Rey F, Petitpas I, Mathieu M, Vaney MC, Cohen J, Kohli E, Pothier P, Hewat E. Antibody inhibition of the transcriptase activity of the rotavirus DLP: a structural view. J Mol Biol 2001;307:161–172.
13. Wiley DC, Skehel JJ. The structure and function of the hemagglutinin membrane glycoprotein of influenza virus. Annu Rev Biochem 1987;56:365–394.
14. Jackson DC, Nestorowicz A. Antigenic determinants of influenza virus hemagglutinin. XI. Conformational changes detected by monoclonal antibodies. Virology 1985;145:72–83.
15. Machius M, Vertesy L, Huber R, Wiegand G. Carbohydrate and protein-based inhibitors of porcine pancreatic alpha- amylase: structure analysis and comparison of their binding characteristics. J Mol Biol 1996;260:409–421.
16. Bompard-Gilles C, Rousseau P, Rouge P, Payan F. Substrate mimicry in the active center of a mammalian alpha-amylase: structural analysis of an enzyme-inhibitor complex. Structure 1996;4:1441–1452.
17. Decanniere K, Desmyter A, Lauwereys M, Ghahroudi MA, Muyldermans S, Wyns L. A single-domain antibody fragment in complex with RNase A: non- canonical loop structures and nanomolar affinity using two CDR loops. Struct Fold Des 1999;7:361–370.
18. Desmyter A, Decanniere K, Muyldermans S, Wyns L. Antigen specificity and high affinity binding provided by one single loop of a camel single-domain antibody. J Biol Chem 2001;276:26285–26290.
19. Decanniere K, Transue TR, Desmyter A, Maes D, Muyldermans S, Wyns L. Degenerate interfaces in antigen-antibody complexes. J Mol Biol 2001;313:473–478.
20. Desmyter A, Transue TR, Ghahroudi MA, Thi MH, Poortmans F, Hamers R, Muyldermans S, Wyns L. Crystal structure of a camel single-domain VH antibody fragment in complex with lysozyme. Nat Struct Biol 1996;3:803–811.
21. Hennecke J, Carfi A, Wiley DC. Structure of a covalently stabilized complex of a human alphabeta T- cell receptor, influenza HA peptide and MHC class II molecule, HLA-DR1. EMBO J 2000;19:5611–5624.
22. Fields BA, Malchiodi EL, Li H, Ysern X, Stauffacher CV, Schlievert PM, Karjalainen K, Mariuzza RA. Crystal structure of a T-cell receptor beta-chain complexed with a superantigen. Nature 1996;384:188–192.
23. Papageorgiou AC, Collins CM, Gutman DM, Kline JB, O'Brien SM, Tranter HS, Acharya KR. Structural basis for the recognition of superantigen streptococcal pyrogenic exotoxin A (SpeA1) by MHC class II molecules and T-cell receptors. EMBO J 1999;18:9–21.
24. Earhart CA, Vath GM, Roggiani M, Schlievert PM, Ohlendorf DH. Structure of streptococcal pyrogenic exotoxin A reveals a novel metal cluster. Protein Sci 2000;9:1847–1851.
25. Thompson JD, Higgins DG, Gibson TJ. CLUSTAL W: improving the sensitivity of progressive multiple sequence alignment through sequence weighting, position-specific gap penalties and weight matrix choice. Nucleic Acids Res 1994;22:4673–4680.
26. Fieulaine S, Morera S, Poncet S, Monedero V, Gueguen-Chaignon V, Galinier A, Janin J, Deutscher J, Nessler, S. X-ray structure of HPr kinase: a bacterial protein kinase with a P-loop nucleotide-binding domain. EMBO J 2001;20:3917–3927.
27. Liao DI, Herzberg O. Refined structures of the active Ser83→Cys and impaired Ser46→Asp histidine-containing phosphocarrier proteins. Structure 1994;2:1203–1216.
28. Fieulaine S, Morera S, Poncet S, Mijakovic I, Galinier A, Janin J, Deutscher J, Nessler S. X-ray structure of a bifunctional protein kinase in complex with its protein substrate HPr. Proc Natl Acad Sci USA 2002;99:13437–13441.
29. Barbey-Martin C, Gigant B, Bizebard T, Calder LJ, Wharton SA, Skehel JJ, Knossow M. An antibody that prevents the hemagglutinin low pH fusogenic transition. Virology 2002;294:70–74.
30. Desmyter A, Spinelli S, Payan F, Lauwereys M, Wyns L, Muyldermans S, Cambillau C. Three camelid VHH domains in complex with porcine pancreatic alpha- amylase. Inhibition and versatility of binding topology. J Biol Chem 2002;277:23645–23650.
31. Sundberg EJ, Li H, Llera AS, McCormick JK, Tormo J, Schlievert PM, Karjalainen K, Mariuzza RA. Structures of two streptococcal superantigens bound to TCR beta chains reveal diversity in the architecture of T cell signaling complexes. Structure (Camb) 2002;10:687–699.
32. Lichtarge O, Bourne HR, Cohen FE. An evolutionary trace method defines binding surfaces common to protein families. J Mol Biol 1996;257:342–358.
33. Heifetz A, Eisenstein M. Effect of local shape modifications of molecular surfaces on rigid-body protein-protein docking. Protein Engineering 2003:16 (in press).